TOP Webinar

On the full-waveform inversion of seismic moment tensors

Antonio André Novotny

Laboratório Nacional de Computação Científica, LNCC/MCTI
Av. Getúlio Vargas 333, 25651-075 Petrópolis - RJ, Brasil

Webinar, March 25^{th}, 2021

Outline

Topological Derivative Concept

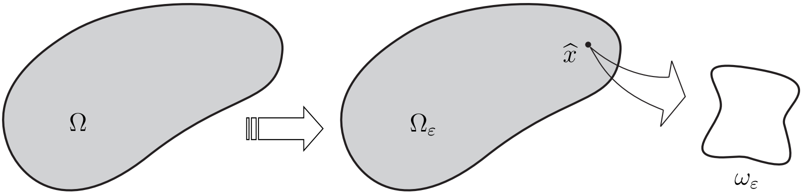

Sokolowski & Zochowski, 1999

$$\psi(\Omega_\varepsilon(\widehat{x})) = \psi(\Omega) + f(\varepsilon)\mathcal{T}(\widehat{x}) + o(f(\varepsilon)) \ ,$$

where $\Omega_\varepsilon(\widehat{x}) = \Omega \setminus \overline{\omega_\varepsilon(\widehat{x})}$ and $f(\varepsilon) \to 0$, when $\varepsilon \to 0$.

Applications of the Topological Derivative Method

$$\mathcal{T}(\widehat{x}) = \lim_{\varepsilon \to 0} \frac{\psi(\Omega_\varepsilon(\widehat{x})) - \psi(\Omega)}{f(\varepsilon)} \ .$$

- Topology Design: Allaire, Amstutz, Canelas, Ferrer, Leugering, Sokolowski, Zochowski ...
- Inverse Problems: Ammari, Bonnet, Capdeboscq, Hrizi, Kang, Laurain, Prakash, Rapún ...
- Multi-Scale Material Design: Giusti, Souza Neto, Toader ...
- Image Processing: Auroux, Belaid, Drogoul, Masmoudi ...
- Fracture and Damage Modeling: Allaire, Jouve, Van Goethem, Xavier ...
- Theory Development: Amstutz, Delfour, Nazarov, Sokolowski ...

Applications of the Topological Derivative Method

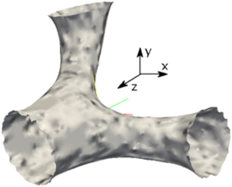

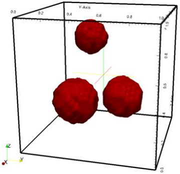

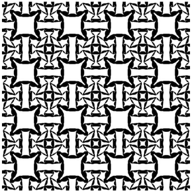

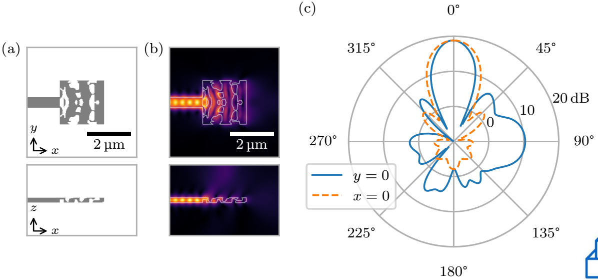

Inverse Seismic Problem

Bojan Guzina

Department of Civil, Environmental & Geo-Engineering,
University of Minnesota, USA

and

Alan Amad

Zienkiewicz Centre for Computational Engineering,
Swansea University Bay Campus, Swansea, Wales, UK

Problem Setting

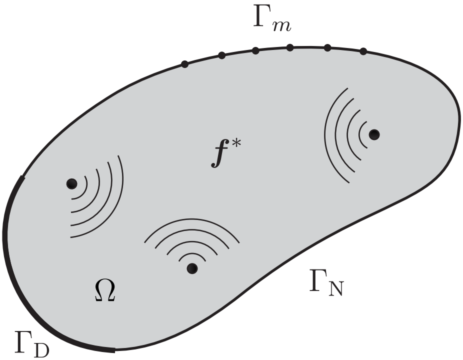

Problem Setting

Find the source term $f^* \in C_\delta(\Omega)$, such that

$$\left\{\begin{array}{rcll} -\mathrm{div}\boldsymbol{\sigma}(z) - \rho\omega^2 z & = & f^* & \text{in} \quad \Omega\,, \\ \boldsymbol{\sigma}(z) & = & \mathbb{D}(\nabla z)^s\,, & \\ z & = & 0 & \text{on} \quad \Gamma_D\,, \\ z & = & u^* & \text{on} \quad \Gamma_m \subset \Gamma_N\,, \\ \boldsymbol{\sigma}(z)n & = & 0 & \text{on} \quad \Gamma_N\,, \end{array}\right.$$

$$C_\delta(\Omega) = \left\{ f : \Omega \to \mathbb{C}^2 \mid f(x) = \sum_{i=1}^{N} M_i \nabla_{x_i} \delta(x - x_i), M_i = M_i^\top \right\},$$

$$\boxed{N^*, M_i^*, x_i^*}$$

Problem Setting

$$\boxed{\Gamma_m \subset \Gamma_N}$$

$$\mathcal{J}(\mathrm{u}) := \frac{1}{2}\int_{\Gamma_m} (\mathrm{u}-\mathrm{u}^*)\cdot\overline{(\mathrm{u}-\mathrm{u}^*)},$$

Find the displacement vector field u, such that

$$\left\{\begin{array}{rcll} -\mathrm{div}\boldsymbol{\sigma}(\mathrm{u}) - \rho\omega^2\mathrm{u} & = & \mathrm{f} & \text{in} \quad \Omega\,, \\ \boldsymbol{\sigma}(\mathrm{u}) & = & \mathbb{D}(\nabla\mathrm{u})^s\,, & \\ \mathrm{u} & = & 0 & \text{on} \quad \Gamma_D\,, \\ \boldsymbol{\sigma}(\mathrm{u})\mathrm{n} & = & 0 & \text{on} \quad \Gamma_N\,, \end{array}\right.$$

Sensitivity Analysis

$$\mathrm{f}_\delta(\mathrm{x}) = \mathrm{f}(\mathrm{x}) + \sum_{i=1}^{N} \mathrm{M}_i \nabla_{\mathrm{x}_i} \delta(\mathrm{x} - \mathrm{x}_i)$$

Find the displacement vector field u_δ, such that

$$\begin{cases} -\mathrm{div}\boldsymbol{\sigma}(\mathrm{u}_\delta) - \rho\omega^2 \mathrm{u}_\delta & = & \mathrm{f}_\delta & \text{in} & \Omega \,, \\ \boldsymbol{\sigma}(\mathrm{u}_\delta) & = & \mathbb{D}(\nabla \mathrm{u}_\delta)^s \,, & & \\ \mathrm{u}_\delta & = & 0 & \text{on} & \Gamma_D \,, \\ \boldsymbol{\sigma}(\mathrm{u}_\delta)\mathrm{n} & = & 0 & \text{on} & \Gamma_N \,. \end{cases}$$

$$\mathcal{J}(\mathrm{u}_\delta) = \frac{1}{2} \int_{\Gamma_m} (\mathrm{u}_\delta - \mathrm{u}^*) \cdot \overline{(\mathrm{u}_\delta - \mathrm{u}^*)}.$$

Sensitivity Analysis

$$
\begin{aligned}
\mathcal{J}(\mathrm{u}_\delta) = \mathcal{J}(\mathrm{u}) &+ \int_{\Gamma_m} \sum_{i=1}^{N} A_i^{kl} \Re\left\{\mathrm{p}_i^{kl} \cdot \overline{(\mathrm{u} - \mathrm{u}^*)}\right\} \\
&- \int_{\Gamma_m} \sum_{i=1}^{N} B_i^{kl} \Im\left\{\mathrm{p}_i^{kl} \cdot \overline{(\mathrm{u} - \mathrm{u}^*)}\right\} \\
&+ \frac{1}{2} \int_{\Gamma_m} \sum_{i=1}^{N} \sum_{j=1}^{N} A_i^{kl} A_j^{mn} \mathrm{p}_i^{kl} \cdot \overline{\mathrm{p}_j^{mn}} \\
&+ \frac{1}{2} \int_{\Gamma_m} \sum_{i=1}^{N} \sum_{j=1}^{N} B_i^{kl} B_j^{mn} \mathrm{p}_i^{kl} \cdot \overline{\mathrm{p}_j^{mn}} \, ,
\end{aligned}
$$

Sensitivity Analysis

$$
\left\{
\begin{array}{rcll}
-\mathrm{div}\boldsymbol{\sigma}(\mathsf{p}_i^{kl}) - \rho\omega^2\mathsf{p}_i^{kl} & = & (\mathsf{e}_k \otimes \mathsf{e}_l)\nabla_i\delta & \text{in} \quad \Omega \, , \\
\boldsymbol{\sigma}(\mathsf{p}_i^{kl}) & = & \mathbb{D}(\nabla\mathsf{p}_i^{kl})^s \, , & \\
\mathsf{p}_i^{kl} & = & 0 & \text{on} \quad \Gamma_D \, , \\
\boldsymbol{\sigma}(\mathsf{p}_i^{kl})\mathsf{n} & = & 0 & \text{on} \quad \Gamma_N \, ,
\end{array}
\right.
$$

$$
\mathsf{M}_i = \mathsf{M}_i^\top \quad \text{and} \quad \mathsf{M}_i = \mathsf{A}_i + \mathrm{i}\mathsf{B}_i
$$

$$
\begin{array}{c}
\alpha_1^i = A_i^{11}, \ \alpha_2^i = A_i^{22}, \ \alpha_3^i = A_i^{12} = A_i^{21}, \\
\beta_1^i = B_i^{11}, \ \beta_2^i = B_i^{22}, \ \beta_3^i = B_i^{12} = B_i^{21}.
\end{array}
$$

Sensitivity Analysis

$$\begin{aligned}\Psi(N,\boldsymbol{\xi},(\boldsymbol{\alpha},\boldsymbol{\beta})) &:= \mathcal{J}(\mathrm{u}_\delta)-\mathcal{J}(\mathrm{u})\\ &= \mathrm{g}\cdot\boldsymbol{\alpha}+\frac{1}{2}\mathrm{H}\boldsymbol{\alpha}\cdot\boldsymbol{\alpha}-\mathrm{h}\cdot\boldsymbol{\beta}+\frac{1}{2}\mathrm{H}\boldsymbol{\beta}\cdot\boldsymbol{\beta}\,,\end{aligned}$$

$$\begin{aligned}\boldsymbol{\xi} &= (\mathrm{x}_1,\ldots,\mathrm{x}_N),\\ \boldsymbol{\alpha} &= (\alpha_1^1,\alpha_2^1,\alpha_3^1,\cdots,\alpha_1^N,\alpha_2^N,\alpha_3^N)^\top,\\ \boldsymbol{\beta} &= (\beta_1^1,\beta_2^1,\beta_3^1,\cdots,\beta_1^N,\beta_2^N,\beta_3^N)^\top.\end{aligned}$$

Reconstruction Algorithm

$$\Psi(N,\boldsymbol{\xi},(\boldsymbol{\alpha},\boldsymbol{\beta})) = \mathrm{g}\cdot\boldsymbol{\alpha} + \frac{1}{2}\mathrm{H}\boldsymbol{\alpha}\cdot\boldsymbol{\alpha} - \mathrm{h}\cdot\boldsymbol{\beta} + \frac{1}{2}\mathrm{H}\boldsymbol{\beta}\cdot\boldsymbol{\beta}\ ,$$

$$\begin{aligned}\langle D_{\boldsymbol{\alpha}}\Psi(N,\boldsymbol{\xi},(\boldsymbol{\alpha},\boldsymbol{\beta});\delta\boldsymbol{\alpha}\rangle &= 0 \quad \forall\delta\boldsymbol{\alpha}\in\mathbb{R}^{3N}\ ,\\ \langle D_{\boldsymbol{\beta}}\Psi(N,\boldsymbol{\xi},(\boldsymbol{\alpha},\boldsymbol{\beta});\delta\boldsymbol{\beta}\rangle &= 0 \quad \forall\delta\boldsymbol{\beta}\in\mathbb{R}^{3N}\ ,\end{aligned}$$

$$\mathrm{H}\boldsymbol{\alpha} = -\mathrm{g} \quad \text{and} \quad \mathrm{H}\boldsymbol{\beta} = \mathrm{h}$$

$$\boldsymbol{\alpha} = \boldsymbol{\alpha}(\boldsymbol{\xi}) \quad \text{and} \quad \boldsymbol{\beta} = \boldsymbol{\beta}(\boldsymbol{\xi})$$

$$\boldsymbol{\xi}^\star = \underset{\boldsymbol{\xi}\in\mathrm{X}}{\operatorname{argmin}}\left\{\Psi(N,\boldsymbol{\xi},(\boldsymbol{\alpha}(\boldsymbol{\xi}),\boldsymbol{\beta}(\boldsymbol{\xi}))) = \frac{1}{2}(\mathrm{g}\cdot\boldsymbol{\alpha}(\boldsymbol{\xi}) - \mathrm{h}\cdot\boldsymbol{\beta}(\boldsymbol{\xi}))\right\}$$

$$\boxed{\boldsymbol{\alpha}^\star = \boldsymbol{\alpha}(\boldsymbol{\xi}^\star) \quad \text{and} \quad \boldsymbol{\beta}^\star = \boldsymbol{\beta}(\boldsymbol{\xi}^\star)}$$

Reconstruction Algorithm

Complexity

$$\mathcal{C}(M,N) = \left(\begin{array}{c} M \\ N \end{array}\right) N^3 = \frac{M!}{N!(M-N)!} N^3$$

where M is the cardinality of the set of admissible locations X and N is the number of trial faults.

Reconstruction Algorithm

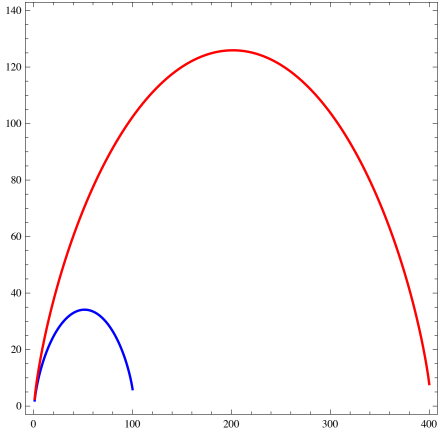

$N \times \log_{10}(\mathcal{C}(M, N))$, for $M = 100$ in blue and $M = 400$ in red

Numerical Examples

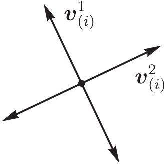

(a) cavitarion

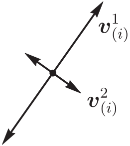

(b) tensile

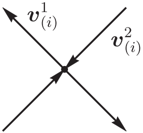

(c) shear

Figure: Graphic representation of the moment tenosr $\boldsymbol{M}_i$

Numerical Examples

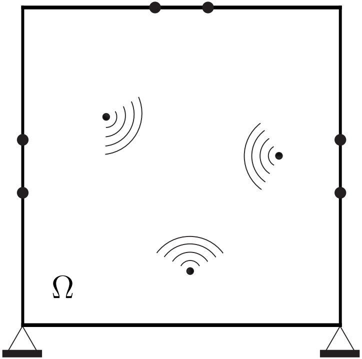

Figure: Specimen

Numerical Examples

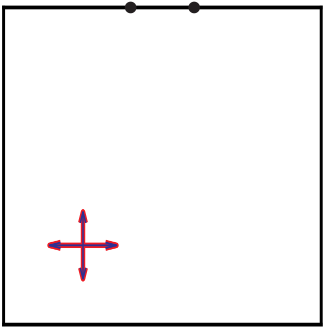

(a) Real Part

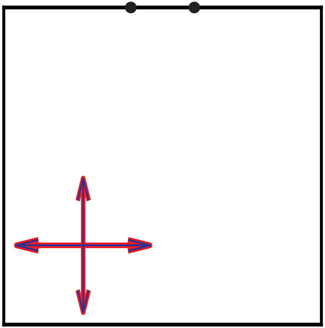

(b) Imaginary Part

Figure: Reconstruction of a single micro-seismic source.

Numerical Examples

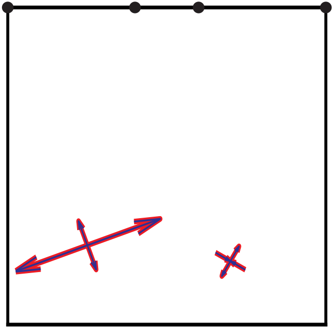

(a) Real Part

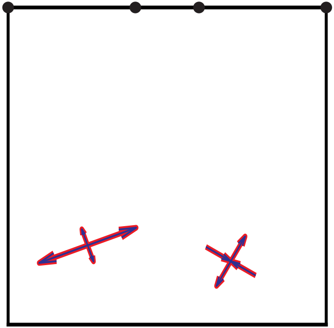

(b) Imaginary Part

Figure: Reconstruction of a pair of micro-seismic sources.

Numerical Examples

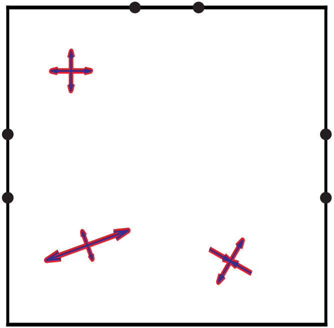

(a) Real Part

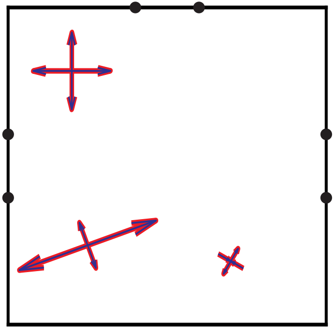

(b) Imaginary Part

Figure: Reconstruction of a triplet of micro-seismic sources.

Numerical Examples

Reconstruction under random modeling errors

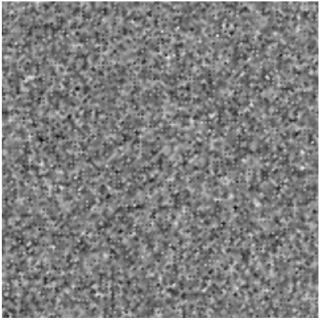

Figure: Corrupted background with White Gaussian Noise (WGN)

Numerical Examples

Reconstruction of a single (mode II) micro-seismic source

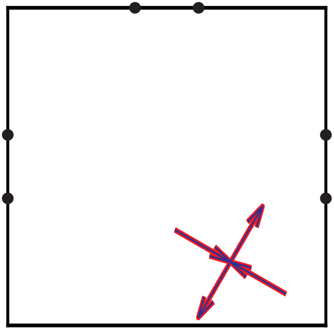

(a) Real Part

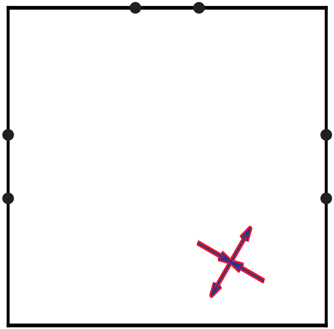

(b) Imaginary Part

Figure: WGN $= 0\%$, $N = 2$

Numerical Examples

Reconstruction of a single (mode II) micro-seismic source

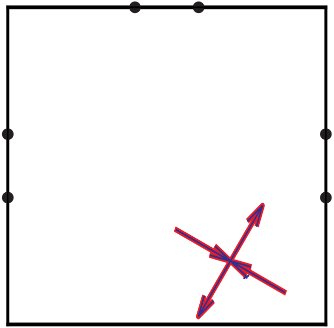

(a) Real Part

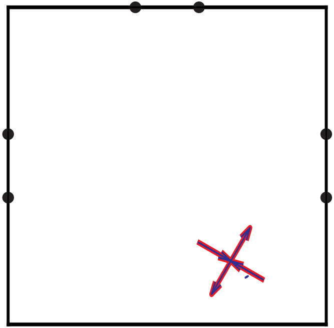

(b) Imaginary Part

Figure: WGN $= 10\%$, $N = 2$

Numerical Examples

Reconstruction of a single (mode II) micro-seismic source

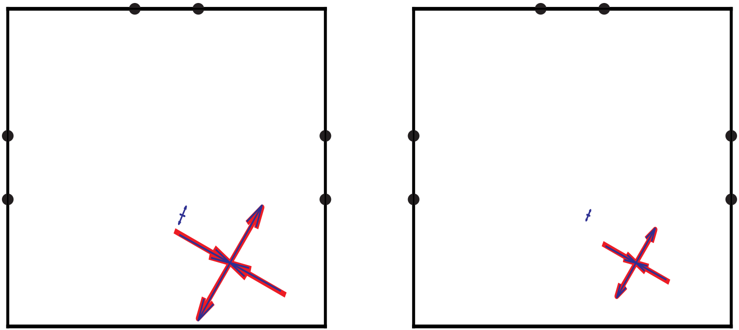

(a) Real Part

(b) Imaginary Part

Figure: WGN $= 21\%$, $N = 2$

Numerical Examples

Reconstruction of a single (mode II) micro-seismic source

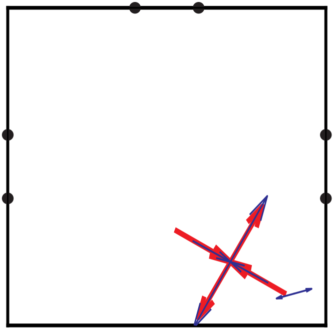

(a) Real Part

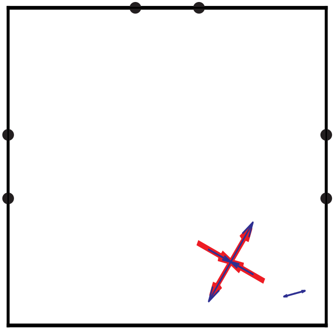

(b) Imaginary Part

Figure: WGN $= 51\%$, $N = 2$

Numerical Examples

Reconstruction of a triplet of micro-seismic sources

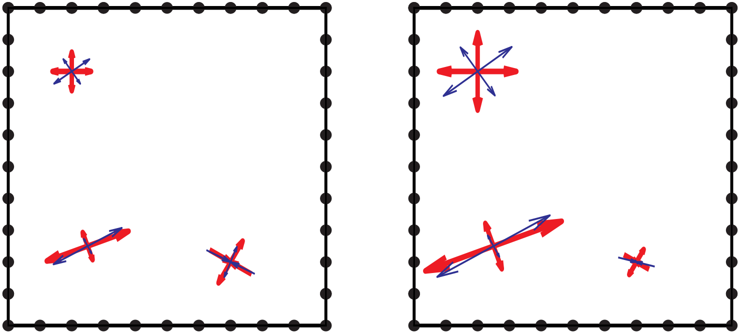

(a) Real Part (b) Imaginary Part

Figure: WGN $= 21\%$, $N = 3$

Numerical Examples

Reconstruction of a triplet of micro-seismic sources

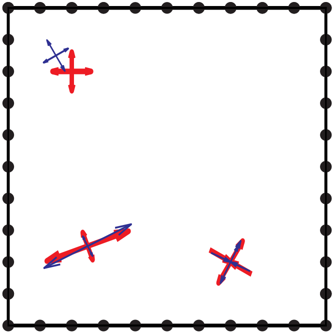

(a) Real Part

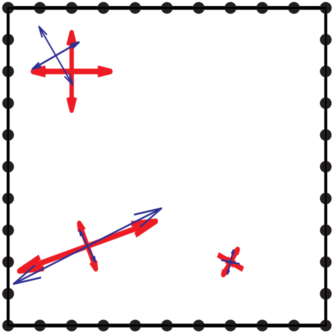

(b) Imaginary Part

Figure: WGN = 36%, $N = 3$

Conclusions

In this work, the full-waveform inversion of seismic point sources in terms of event locations and seismic moment tensors has been investigated. The novelty of the proposed methodology resides in a hybrid grid search for micro-seismic source locations that encapsulates the optimality condition on the respective moment tensors. The significance of the proposed frequency domain algorithm is three-fold:

1. it allows for the reconstruction of non-synchronous seismic sources, i.e. micro-fractures whose seismic moment tensor may evolve (in terms of eigenvalues and eigenvectors) during the fracture creation process;
2. it permits simultaneous (location and moment tensor) reconstruction of multiple point sources, which in physical terms allows for several micro-seismic events to overlap in time; and
3. the resulting reconstruction algorithm is non-iterative and thus very resilient with respect to noisy data.

Thank you very much!

https://novotny.lncc.br